Food and Chemical Toxicology 125 (2019) 150–160

Contents lists available at ScienceDirect

Food and Chemical Toxicology

journal homepage: www.elsevier.com/locate/foodchemtox

Immunomodulatory activity of marine natural products: Synthesis, spectral characterization and toxicity assessment of natural and related synthetic iodinated tyramides

Miljana R. Đorđević[a], Niko S. Radulović[a,*], Nikola M. Stojanović[b], Pavle J. Ranđelović[c]

[a] Department of Chemistry, Faculty of Sciences and Mathematics, University of Niš, Višegradska 33, 18000, Niš, Serbia
[b] Faculty of Medicine, University of Niš, Dr Zoran Đinđić Boulevard 81, 18000 Niš, Serbia
[c] Department of Physiology, Faculty of Medicine, University of Niš, Dr Zoran Đinđić Boulevard 81, 18000 Niš, Serbia

ARTICLE INFO

Keywords:
N-(3,5-diiodo-4-methoxyphenethyl)benzamide
Ascidian
Toxicity
Artemia salina
Macrophages
Immunomodulatory activities

ABSTRACT

The toxicity of natural marine iodoarenes or their synthetic counterparts is widely unknown despite the fact that triiodothyronine and thyroxine are members of this class. In this work we aimed to expand such knowledge on iodinated marine natural products and tested an ascidian (*Didemnum rubeum*) metabolite, *N*-(3,5-diiodo-4-methoxyphenethyl)benzamide, together with closely related synthetic iodinated tyramides: *N*-(2,5-diiodo-4-methoxyphenethyl)benzamide, *N*-(3-iodo-4-methoxyphenethyl)benzamide, *N*-(4-methoxyphenethyl)benzamide, and *N*-(3-iodo-4-methoxyphenethyl)formamide, for their effect on the viability of rat macrophages, as well as acute toxicity on *Artemia salina*. The tested tyramides exerted a varying degree of toxicity towards brine shrimps, but in certain cases, the determined lethal concentrations were even lower than those of known toxicants (e.g. strychnine sulfate, SDS). The toxicity was highly dependent on the structure of these mutually related compounds, while the natural one was shown to be the most toxic. In the case of macrophage cultures, the tested tyramides exerted much less toxicity but were found to have an effect on the functioning of these normal immune cells. The samples of the tyramides were obtained by synthesis, and were fully structurally and spectrally characterized, which also provided corroboration of the proposed structure of the natural product originally isolated in minute amounts.

1. Introduction

Ascidians (Tunicates; Ascidiacea), also known as tunicates, are among the most frequently investigated groups of marine organisms with about 3000 reported living species (Shenkar and Swalla, 2011; Davidson, 1993). A number of tunicates, wild-harvested or cultured, are a part of the human diet in different parts of the world, including some European countries (Abdul Jaffar Ali and Tamilselvi, 2016; Lambert et al., 2016), where they are regarded as healthy seafood high in protein and low in calories. These marine invertebrate filter feeders use secondary metabolites for protection against predators and microbial pathogens, as well as intra- or interspecies interactions (Palanisamy et al., 2017). It is no wonder that ascidians represent an unusually rich source of bioactive secondary metabolites (Sri Kumaran et al., 2011). Up to now, most of the studies of their biological activities were oriented towards the discovery of novel cytotoxic or antibiotic agents (Palanisamy et al., 2017; Watters, 2018). Ascidian metabolites (and their analogs) found clinical usage in advanced soft-tissue sarcoma, osteosarcoma, metastatic breast cancers (Yondelis® - trabectedin and Aplidin® - dehydrodidemnin B, respectively) (Fayette et al., 2005; González-Santiago et al., 2006). Most of these bioactive metabolites are amino acid-derived compounds of varying complexity: from oligopeptides to simple derivatives of a single (non-essential) amino acid.

Halogenated metabolites are a characteristic of marine organisms, including ascidians, and are known to commonly include chlorine and bromine, while only a small number of iodine-containing metabolites were identified (Murphy, 2003). Iodinated natural compounds have been divided (Borrelli et al., 2004) into five general classes of compounds: 1) volatile ones such as iodomethane (Itoh et al., 1997), 2) terpene derivatives (Williams et al., 2003), 3) fatty acid-related compounds (Dugrillon and Gaetner, 1995), 4) nucleoside derivatives (Kazlauskas et al., 1983), and 5) tyrosine-related compounds (Kigoshi et al., 1999). Among the classes, the most renown and perhaps biologically most investigated, is the last one, with thyroxine and related compounds as flagpoles. Expressed through their cytotoxic effect on transformed cells, i.e. various kinds of cancer cell lines, halogenated

* Corresponding author. Department of Chemistry, Faculty of Sciences and Mathematics, University of Niš, Višegradska 33, 18000 Niš, Serbia.
E-mail address: nikoradulovic@yahoo.com (N.S. Radulović).

https://doi.org/10.1016/j.fct.2018.12.039
Received 1 November 2018; Received in revised form 21 December 2018; Accepted 22 December 2018
Available online 24 December 2018
0278-6915/

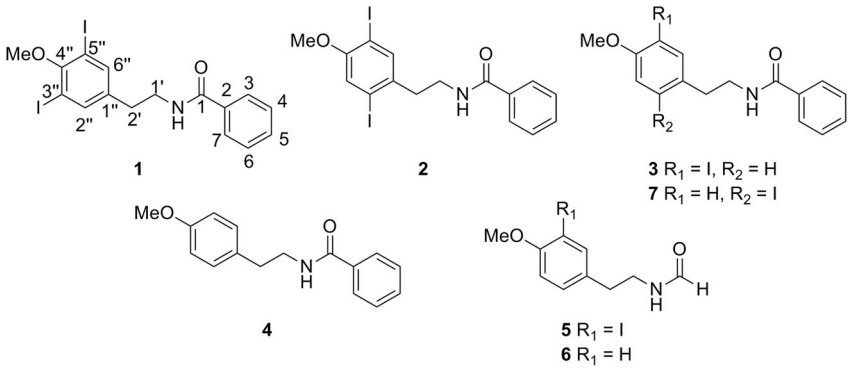

Fig. 1. Structures of compounds **1–7**: *N*-(3,5-diiodo-4-methoxyphenethyl)benzamide (**1**), *N*-(2,5-diiodo-4-methoxyphenethyl)benzamide (**2**), *N*-(3-iodo-4-methoxyphenethyl) benzamide (**3**), *N*-(4-methoxyphenethyl)benzamide (**4**), *N*-(3-iodo-4-methoxyphenethyl)formamide (**5**), *N*-(4-methoxyphenethyl)formamide (**6**), and *N*-(2-iodo-4-methoxyphenethyl)benzamide (**7**); compounds **1–5** were assessed for immunomodulatory activity.

amino acid derivatives have been acclaimed with immunomodulatory activities (Won et al., 2015; Carroll et al., 1993; Aiello et al., 2010). However, little or nothing is known on the effect of these compounds or even crude extracts thereof on the viability and functioning of immune cells, such as macrophages. Among the rare studies that dealt with this subject, the report of Ananthan and Iyappan (2014) demonstrated an effect of a crude ethanolic extract of an ascidian, *Didemnum albidum*, on the human monocytic cell line. There are sporadic studies of the effects of secondary metabolites from other ascidians (other genera) on macrophages (Palanisamy et al., 2017; Coombe et al., 1981).

Recently, motivated by the alleged (stated, but data not provided) cytotoxic activity of the crude water extract of tunicate *Didemnum rubeum*, Solano et al. (2009) isolated and structurally elucidated seven iodinated tyramine derivatives. Having only minute quantities of the isolated compounds in their hands, in the cases of some metabolites, the researchers had to use spectral data from HSQC and HMBC experiments to extract ^{13}C NMR resonances, and were unable to perform any further biological tests to ascertain the carrier of the original cytotoxic nature of the water extract. One should note that the structures of these metabolites (for example compound **1**, Fig. 1) contain an iodinated methoxyaryl group reminiscent of thyroxine. With an aim to provide a definitive proof of the structures of some of these *Didemnum* metabolites, and to allow access to larger amounts of these compounds, we set ourselves to a synthetic endeavor to prepare compounds **1–5**, that either represent a natural compound (**1**) identified in this tunicate, or are isomers (**2**), or closely related compounds to the ones naturally occurring (**3** and **4** are related to benzamides, **5** is related to formamide).

Target compounds were chosen to enable an assessment of the structure-activity/toxicity relationship in the case of their possible immunomodulatory activity effectuated through their effect on rat macrophages viability and function. This cytotoxic activity could be expected based on the previous findings of the cytotoxic nature of the water extract of this ascidian (Solano et al., 2009) and the previously mentioned effect on macrophages of an ethanolic extract of another *Didemnum* sp. (Ananthan and Iyappan, 2014). Very recently, compound **1** and related unnatural derivatives, differing in the identity of the substituted benzoic acid moiety, were synthesized and *in vitro* screened for their cytotoxic activity against U-937 macrophages and *Plasmodium falciparum*, *Leishmania panamensis* and *Trypanosoma cruzi* protozoan parasites (Restrepo et al., 2019). Also, in the same study (Restrepo et al., 2019), these iodinated tyramides were demonstrated not to possess hemolytic activity (human red blood cells).

Having all of the above in mind, in this paper, we report the total synthesis and full structural characterization of compounds **1–5** (Fig. 1), and also present their immunomodulatory activities. Two more related derivatives, **6** and **7**, were also fully spectrally characterized but were not tested. To the best of our knowledge, compounds **2**, **3**, **5**, and **7** are completely new compounds. In addition to the tests with rat macrophages, all of the compounds were also screened for their acute toxicity in the model of *Artemia salina*. By doing this we hope to enlarge the body of toxicological data on the metabolites of these tunicates that are potentially part of the human sustenance.

2. Results and discussion

2.1. Chemistry

Herein, we report a new synthesis of the natural product, **1**, and of its analogs (**2–7**), Fig. 1. According to a search of the CAS database (SciFinder, accessed on October 2018) compounds **2**, **3**, **5** and **7** represented new compounds. Interestingly, to the best of our knowledge, complete experimental data (NMR spectra, IR and MS) of **6** do not exist in the literature. Our synthetic plan for *N*-(3,5-diiodo-4-methoxyphenethyl)benzamide (**1**) and related iodinated tyramides is illustrated in Fig. 2. The syntheses of the target natural compound **1** and its analogs were commenced with a carbodiimide-facilitated coupling procedure utilizing commercially available 2-(4-methoxyphenyl)ethanamine and the appropriate carboxylic acids (benzoic or formic) (Pfaffenbach and Gaich, 2015). The resulting amides **4** and **6** were subjected to iodination in two stages.

The first stage afforded intermediary organomercury compounds, which involved mercuration of **4** and **6** with mercury(II) acetate. In the second stage, following an exchange of the acetate ligands with chlorides, Hg-C bond was cleaved by the action of elemental iodine resulting

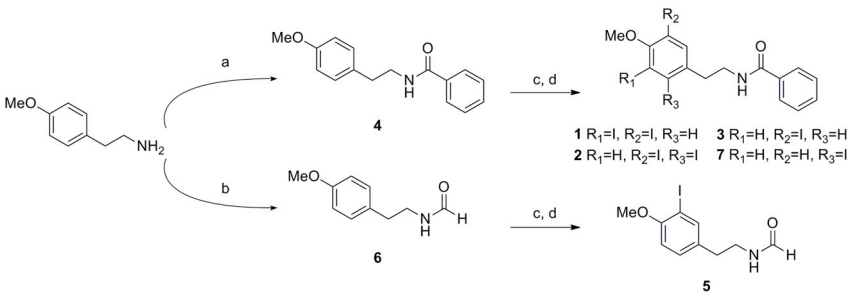

Fig. 2. Synthesis of compounds **1–7**. Reagents and conditions: (a) 1.5 eq benzoic acid, 1.5 eq DCC, 3–10 mol% DMAP, CH_2Cl_2, rt, 5 h; (b) 1 eq formic acid, 1.1 eq DCC, 3–10 mol% DMAP, CH_2Cl_2, rt, 5 h; (c) $Hg(OAc)_2$, 70% $HClO_4$, glacial CH_3COOH, rt, 48 h; (d) NaCl, H_2O, 30 min; I_2, CH_2Cl_2 (dry), 16 h.

Table 1
^{1}H NMR data (at 400 MHz, recorded in $CDCl_3$) for compounds **1–7**.

Position	1	2	3	4	(*Z*)-5	(*E*)-5	(*Z*)-6	(*E*)-6	7
	δ_H (*J* in Hz)	δ_H (*J* in Hz)	δ_H (*J* in Hz)	δ_H (*J* in Hz)	δ_H (*J* in Hz)	δ_H (*J* in Hz)	δ_H (*J* in Hz)	δ_H (*J* in Hz)	δ_H (*J* in Hz)
1					8.12, *s*	7.89, d (9.4)	8.08, *s*	7.84, d (11.9)	
2									
3, 7	7.72, m	7.74, m	7.71, m	7.70, m					7.72, m
4, 6	7.43, m	7.43, m	7.41, m	7.40, m					7.42, m
5	7.50, m	7.50, m	7.49, m	7.48, m					7.51, m
1′	3.63, td (7.1, 6.0)	3.65, td (7.0, 6.0)	3.65, td (6.9, 5.9)	3.67, td (6.9, 5.9)	3.51, td (7.0, 6.2)	3.43, td (7.0, 6.3)	3.51, td (7.0, 5.9)	3.41, td (6.8, 6.4)	3.68, td (7.0, 6.2)
2′	2.82, t (7.0)	2.99, t (7.0)	2.84, t (6.9)	2.87, t (6.9)	2.75, t (7.0)	2.73, t (7.0)	2.77, t (7.0)	2.74, t (6.8)	3.02, t (7.0)
1″									
2″	7.64, br *s*		7.66, d (2.1)	7.15, m	7.62, d (1.9)	7.60, d (1.7)	7.11, m	7.08, m	
3″		7.20, *s*		6.86, m			6.84, m		7.38, d (2.6)
4″									
5″			6.77, d (8.3)	6.86, m	6.77, d (8.3)	6.85, d (8.5)	6.84, m		6.86, dd (8.4, 2.6)
6″	7.64, br *s*	7.54, br *s*	7.17, dd (8.3, 2.1)	7.15, m	7.15, dd (8.3, 1.9)	7.12, dd (8.2, 1.7)	7.11, m	7.08, m	7.14, d (8.4)
NH	6.31, br t (5.2)	6.23, br t (5.3)	6.27, br t (5.3)	6.28, br t (5.3)	5.95, br *s*	6.02, br *s*	6.0, br *s*	6.07, br *s*	6.26, br t (6.3)
OCH_3	3.84, *s*	3.86, *s*	3.86, *s*	3.79, *s*	3.86, *s*		3.78, *s*		3.77, *s*

in the replacement of the –HgCl group with an iodine atom. Initially, all reaction mixtures were analyzed by GC-MS, and the TIC chromatograms displayed four peaks, two belonging to monoiodinated tyramides, and two originating from diiodinated derivatives, as inferred from their mass spectra. In the case of benzamide iodination, the resulting mixture of mono- and diiodinated products was straightforwardly separated by SiO_2 chromatography. The major product was the monoiodinated derivative **3** with the iodine atom introduced *ortho* to the methoxy group obtained in 43% yield. The only other possible monoiodinated derivative (**7**), I *ortho* to CH_2, also formed but was isolated in minute quantities (ca. 1%) that permitted us to confirm its identity by NMR but the amount was insufficient for any biological tests. The diiodinated products, two regioisomers (**2**, and the natural isomer **1**), were obtained in approximately equal yields (ca. 15%). In both isomers, one iodine atom was *ortho* to the more electron donating MeO- group, while the other entered either also *ortho* to MeO- (**1**) or went *para* to the mentioned iodine (**2**).

The chromatogram of the formamide iodination reaction mixture suggested that only a single monoiodinated product formed predominantly, while there were three peaks that corresponded to diiodinated formamides. Curiously, after a preparative column chromatography, we were able to obtain only compound **5**, and there were no fractions that contained the diiodinated derivatives. This could have been the outcome of decomposition of these diiodo formamides on silica gel.

The position of the iodine atom(s) in **1–3**, **5**, **7** was(were) unambiguously inferred from their NMR data, presented in Tables 1 and 2, and in addition to these spectral data, compounds **1–3**, and **5** were additionally characterized by IR and UV spectra. A complete assignment of ^{1}H and ^{13}C NMR resonances was accomplished by a detailed analysis of 1D and 2D NMR spectra (a series of selective homonuclear ^{1}H decoupling, and grHSQC, grHMBC, gradient ^{1}H-^{1}H COSY, and NOESY). Several conformational and spectral features of these compounds deserve mention. All ^{1}H and ^{13}C NMR spectroscopic data of compound **5** provided evidence of the presence of two rotameric forms due to a slow rotation (on the NMR time scale) around the amide bond, N–CO (exchange peaks visible in NOESY/ROESY spectra). These species could be completely characterized, while their ratio in $CDCl_3$ at 25 °C, based on the integration of well-separated signals in the ^{1}H NMR spectrum, was 1: 5.56 in favor of the *Z*-rotamer (*antiperiplanar* conformer, Fig. 3). The major rotamer displayed a broad singlet formyl proton signal, whereas the minor (*synperiplanar* conformer) isomer gave a doublet with $J = 9.4$ Hz for the same proton in agreement with the higher expected coupling expected for an antiperiplanar orientation of the HN–CH fragment. The non-iodinated formamide **6** showed a related conduct to that of **5**. Such conformational behavior might be of importance due to two available conformations with possible differential interaction(s) with the biological target molecule. The HSQC signal of C1-H1 (within the carbonyl) of the *Z*-rotamers of **5** (Fig. 3) and **6** appeared as “multiplets” (quartet-like) having the two farthest peaks corresponding to a $^1J_{CH}$ doublet (192.8 and 192.5 Hz, respectively; these precise values were determined from ^{1}H coupled ^{13}C NMR spectra), while the *E*-rotamers were broadened doublets having a splitting that is considerably lower than the measured $^1J_{CH}$ (189.3 and 188.7 Hz, respectively; values from ^{1}H coupled ^{13}C NMR spectra). These are probably artifacts due to a significant mismatch of d2, and/or d4 delays, optimized to $^1J_{CH} = 145$ Hz, for the one-bond coupling of formamide ^{1}H/^{13}C nuclei in question. The value of the one-bond coupling constant is proportional to the bond order (electron density between the two atoms). One can expect different electron densities in the two rotamers and therefore different values of $^1J_{CH}$.

HMBC spectra of **1**, **3** and **5** contained cross-peaks that were only assignable to a four-bond coupling between an Ar-H proton and an ArC-I carbon atom *para* to the hydrogen. This was also evident from the ^{1}H-coupled ^{13}C NMR spectra where, in the case of the monoiodinated derivatives **3** and **5**, the carbon directly bonded to iodine appeared as a

Table 2
^{13}C NMR data (at 100.6 MHz recorded in $CDCl_3$) for compounds **1–7**.

Position	1	2	3	4	(*Z*)-5	(*E*)-5	(*Z*)-6	(*E*)-6	7[a]
	δ_C (*J* in Hz)	δ_C (*J* in Hz)	δ_C (*J* in Hz)	δ_C (*J* in Hz)	δ_C (*J* in Hz)	δ_C (*J* in Hz)	δ_C (*J* in Hz)	δ_C (*J* in Hz)	δ_C (*J* in Hz)
1	167.81, m	167.81, m	167.66, m	167.57, m	161.34, br d (192.8)	164.59, br d (189.3)	161.35, d ps q (192.5, 3.7)	164.71, dt (188.7, 5.0)	167.71
2	134.48, t (7.5)	134.61, t (7.4)	134.61, t (7.3)	134.70, t (7.2)					134.61
3, 7	126.97, dt (158.38, 7.8)	127.02, br d ps t (159.7, 7.4)	126.93, br d ps t (159.5, 7.1)	126.91, br d ps t (158.5, 6.8)					126.98
4, 6	128.78, dd (161.1, 7.7)	128.75, br dd (161.2, 7.5)	128.71, br dd (161.2, 7.5)	128.65, dd (161.3, 7.7)					128.70
5	131.73, dt (161.2, 7.7)	131.64, dt (161.1, 7.2)	131.60, dt (161.1, 7.4)	131.50, dt (161.1, 7.5)					131.60
1′	41.11, tm (140.3)	40.20, tm (138.8)	41.31, br tm (139.8)	41.43, br tm (140.1)	39.26, tm (140.1)	43.21, tm (139.1)	39.41, tm (139.5)	43.43, tm (138.3)	40.39
2′	34.12, t ps quintet (129.5, 3.2)	38.95, tm (129.5)	34.40, tm (128.8)	34.85, tm (128.1)	34.04, t ps quintet (128.8, 3.2)	36.24, tm (128.4)	34.56, t ps quintet (128.1, 3.3)	36.77, tm (128.4)	39.14
1″	139.05, m	136.03, m	133.16, m	130.93, m	132.63, m	131.71, m	130.49, m	129.61, m	133.65
2″	140.20, ddt (164.7, 7.8, 5.3)	100.07, m	139.73, ddt (162.1, 7.5, 5.4)	129.86, ddt (156.37, 7.5, 5.2)	139.47, ddt (162.2, 7.9, 5.0)	139.51, m	129.68, ddt (156.1, 7.5, 5.1)	129.84, ddt (155.2, 7.2, 5.1)	100.52
3″	90.76, ps t (2.2)	121.66, d (165.0)	86.21, ddd (7.7, 2.9, 1.8)	114.16, dm (158.4)	86.06, ddd (7.7, 2.7, 1.7)	86.26, br d (7.7)	114.07, dm (158.3)	114.21, dm (158.1)	124.70
4″	157.60, m	157.34, m	156.93, m	158.34, m	156.82, m	158.25, m	158.31, m	158.47, m	158.62
5″	90.76, ps t (2.2)	86.22, dd (7.8, 3.2)	111.07, br d (159.4)	114.16, dm (158.4)	110.94, br d (159.4)	114.03, dm (163.2)	114.07, dm (158.3)	114.21, dm (158.1)	114.75
6″	140.20, ddt (164.7, 7.8, 5.3)	139.76, dt (164.8, 5.5)	129.95, ddt (160.8, 7.5, 5.0)	129.86, ddt (156.4, 7.5, 5.2)	129.80, ddt (158.1, 7.3, 5.0)	130.03, ddt (158.5, 6.9, 5.1)	129.68, ddt (156.1, 7.5, 5.1)	129.84, ddt (155.2, 7.2, 5.1)	130.33
O<u>C</u>H$_3$	60.86, q (145.6)	56.80, q (145.2)	56.50, q (144.7)	55.37, q (143.7)	56.39, q (144.6)		55.26, q (143.6)		55.64

The following abbreviations were used to designate multiplicities: br, broad signal; ps, pseudo; s, singlet; d, doublet; t, triplet; q, quartet; dd, doublet of doublets; dt, doublet of triplets; ddt, doublet of doublet of triplets; td, triplet of doublets; m, multiplet; dm, doublet of multiplets; tm, triplet of multiplets.

[a] ^1H-coupled ^{13}C spectrum of compound **7** was not recorded due to a small amount of the substance available.

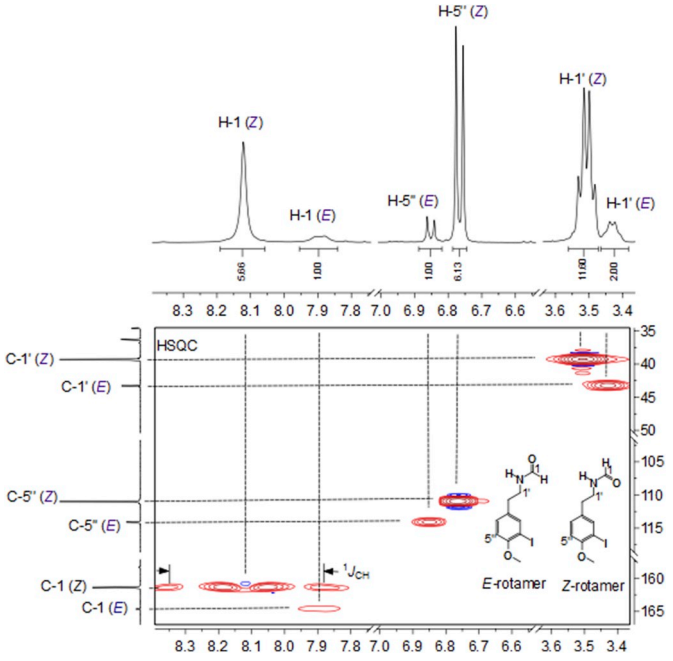

Fig. 3. Expansions of the ^{1}H NMR and grHSQC spectra of compound **5** showing the presence of two rotamers (designated as *E* and *Z*) around the amide bond, N–CHO.

ddd multiplet with ^{3}J = 7.7 Hz, and ^{2}J and ^{4}J were around 2.6–2.9 Hz and 1.4–1.7 Hz, respectively, while in compound **1** the corresponding signal was a pseudotriplet with similar ^{2}J and $^{4}J \approx$ 2.2 Hz. We previously encountered this long-range coupling apparently facilitated by the iodine atom in a series of iodinated dehydrodithymols and the related parent iodinated thymols (Radulović et al., 2016a).

We attempted an alternate synthetic methodology, that avoids mercuration altogether, centered on a Henry reaction of an appropriately substituted benzaldehyde derivative **9** (cf. Supplementary data file) with nitromethane, however, the reduction of the obtained nitrostyrene **10** was unsuccessful either directly, with $LiAlH_4$ or catalytic hydrogenation, to the diiodinated-*O*-methyl-tyramine or stepwise ($NaBH_4$) via the saturated nitro-compound **11**. $LiAlH_4$ reduced the nitrostyrene to the phenethylamine but also dehalogenated the core. A similar outcome was noted in the case of the reduction of **11** with $LiAlH_4$. Pd/C did not catalyze the hydrogenation, and the starting material was reisolated from the reaction mixtures.

2.2. Toxicological and pharmacological properties

2.2.1. Brine shrimp toxicity

The natural compound (**1**), and the related iodinated (**2**, **3** and **5**) and non-iodinated (**4**) tyramides were screened for their acute toxicity in an *Artemia salina* (brine shrimp) lethality assay (Radulović et al., 2013), in concentrations ranging from 1 to 200 μM. Based on the survival of nauplii after 24 h of incubation with the test substances, compounds **3** and **4** exerted the strongest toxic effect, higher than that of the naturally occurring **1** (Table 3). The 24 h-toxicity was found to decrease in the following order: **3** > **4** > **1** > **2** > **5**, while the order changed after a prolonged incubation period (48 h): **1** > **3** > **4** > **2** > **5**, with compound **1** as the most toxic one ($LD_{50\ (after\ 48h)}$ = 20 μM). It appears that benzamides (**1–4**) exerted a more toxic effect compared to the only formamide tested **5**. The presence and regiochemistry of iodine atoms on the tyramine core seem to play a role in the toxic profile but does not seem to be apparently regular. If two iodine atoms were required for a more pronounced toxicity then compound **2** should also be more toxic than **3** and **4**, and this is not the case. The complete absence of iodine in **4** did not result in any significant drop in toxicity since this compound was among the most toxic ones. When compared to the positive control ($LD_{50\ (after\ 24\,h)}$ = 147.5 μM; literature values in the range 49–122 μM (Toğulga, 1998), compounds **1–5** all displayed a more pronounced toxicity after 24 h of treatment and were more toxic or comparable to SDS after 48 h of incubation with the test substances. It is worth mentioning that the benzamides are all more toxic than strychnine sulfate ($LD_{50\ (after\ 24\,h)}$ ca. 100 μM, Meyer et al., 1982) in this particular assay. Ephedrine sulfate, a structurally closer phenethylamine derivative, was found to have $LD_{50\ (after\ 24\,h)}$ ca. 500 μM (Meyer et al., 1982) which is an order of magnitude less toxic effect than that of compounds **3** ($LD_{50\ (after\ 24h)}$ = 50 μM). As mentioned above, Ananthan et al. (2011) previously reported a toxic activity of the crude extracts of *Didemnum psammatodes* in the *A. salina* nauplii model, which is in agreement with the current results.

2.2.2. Effects of compounds 1–5 on macrophage viability

To assess the *in vitro* cytotoxic activity of compounds **1–5**, rat peritoneal macrophages (Mφ) were treated with these compounds for 24 h, and cell viability was determined using the MTT assay. Tested in a broad range of concentrations (10^{-7}–$5x10^{-4}$), compounds **1**, **3** and **5** (at 10^{-4}–$5x10^{-4}$ moldm^{-3}) caused a statistically significant decrease in Mφ viability in the MTT assay (Fig. 4). Compounds **2** and **4** were found not to statistically alter Mφ viability in the tested concentration range. The highest tested concentration of compound **5**, 5×10^{-4} moldm^{-3}, showed Mφ viability reduction of *ca.* 50%, whereas cisplatin, at 10^{-4} moldm^{-3}, caused a 40% decrease of viability (Fig. 4). It is interesting to note that all of the tested tyramides displayed their effect in a relatively narrow concentration range (10^{-4}–$5x10^{-4}$ moldm^{-3}), and no cytotoxic effects were observed for lower tested concentrations. When compared to the previously determined LC_{50} of compound **1** (65 μmoldm^{-3}) in the case of human U-937 macrophages (Restrepo et al., 2019), it appears that the rat macrophages are less sensitive to the action of compound 1 (our LC_{50} was around 250 μmoldm^{-3}). Other tested related unnatural derivatives having a methyl, methoxy or a nitro para-substituent on the benzoic acid moiety were of comparable toxicity to the unsubstituted one (Restrepo et al., 2019).

A consideration of the structures of the tested tyramides and those from the literature (Restrepo et al., 2019) suggests that the presence of iodine is necessary for a pronounced decrease in the cellular reduction

Table 3
Acute toxicity of *N*-(3,5-diiodo-4-methoxyphenethyl)benzamide (**1**), *N*-(2,5-diiodo-4-methoxyphenethyl)benzamide (**2**), *N*-(3-iodo-4-methoxyphenethyl)benzamide (**3**), *N*-(4-methoxyphenethyl)benzamide (**4**), *N*-(3-iodo-4-methoxyphenethyl)formamide (**5**), and SDS (positive control) in *Artemia salina* (brine shrimps).

Compound	LD_{50} (μmol/L, after 24 h)	LD_{50} (μmol/L, after 48 h)
N-(3,5-diiodo-4-methoxyphenethyl)benzamide (**1**)	100.0	20.0
N-(2,5-diiodo-4-methoxyphenethyl)benzamide (**2**)	145.0	100.0
N-(3-iodo-4-methoxyphenethyl)benzamide (**3**)	50.0	36.6
N-(4-methoxyphenethyl)benzamide (**4**)	83.5	56.5
N-(3-iodo-4-methoxyphenethyl)formamide (**5**)	> 200.0	> 200.0
Sodium dodecyl sulfate (SDS)	147.5	92.2

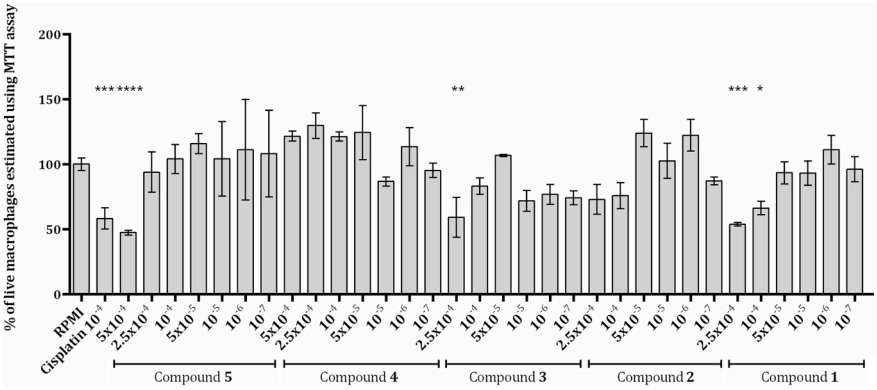

Fig. 4. The effects of compounds **1–5** (in moldm^{-3}) on macrophage viability based on the MTT assay. Data are presented as mean ± S.D. The statistical significance was calculated by one-way ANOVA followed by Dunnett's post-hoc test. *p < 0.05, **p < 0.01, ***p < 0.001 and ****p < 0.0001 vs. RPMI medium-treated cells.

capacity as measured by the MTT assay (compound **4** was devoid of any apparent toxicity); however the position of the iodine atom on the aromatic core of tyramine is also important (all derivatives having I atom(s) *ortho* to the OMe group displayed an effect on the reducing cellular capacity, frequently associated with Mφ mitochondria functioning, except for the derivative that also had an I atom *ortho* to the CH_2CH_2 tether). Going from a benzamide to a formamide had little or no result of the toxicity of the tyramides. We might speculate that the observed activity of the tested compounds might be the consequence of metabolites that are formed from the tyramide derivatives; our guess is that after the initial hydrolysis (hence the amide identity is of little importance), the phenethylamines undergo further metabolism to hydroxylamines or oximes (Irsfeld et al., 2013), that either act as possible mitochondrial toxicants, or are converted to the corresponding aldehydes (Suzuki et al., 1981). Thus, an *ortho* voluminous group to the site of these oxidations would hamper the formation of these possibly more toxic metabolites.

2.2.3. *Effects of compounds **1–5** on macrophage functional properties*

We also evaluated the effect of compounds **1–5** on the ability of Mφs to accumulate neutral red (NR). Viable cells uptake and accumulate the weakly basic dye NR into their lysosomes, and any destabilization in the lysosomal membrane results in the reduction of NR retention inside the lysosomes (Radulović et al., 2016b). After a 24-h incubation period with increasing concentrations of compounds **1–3** and **5**, Mφs showed no statistically significant alteration in the accumulation of NR. However, compound **4** lead to a statistically significant reduction of the uptake of NR in all tested concentrations (Fig. 5). If we bear in mind the results from the MTT and NR tests, we can see that compound **4** did not affect the activity of Mφ mitochondria, i.e. the reducing cellular capacity, while it significantly reduced the dye uptake. Thus, the observed reduction in the phagocytic function is not the result of a decrease in the number of Mφ but a specific effect on Mφ lysosomes. Hence, by exerting an effect on the phagocytosis and/or phagolysosome involving processes, in all tested concentrations while not affecting Mφ viability, compound **4** could be classified as being immunomodulatory, and such activity (effect) can be beneficial in situations of immune system overactivation. One might also notice that there is an apparent increase in the uptake of NR by Mφ that were treated with the natural product **1**, that showed a decrease in cellular reduction capacity (MTT assay) at the highest tested concentration. Thus, it might be that the more active tyramide derivatives additionally increase the lysosome ability to retain NR.

In order to investigate the influence of compounds **1–5** on the adherence ability of Mφs, a methylene-blue assay was performed (Radulović et al., 2017). The adhesion of Mφs represents one of their main functions in providing a defense role in the organism. Therefore, any disruption in this property would result in a reduced function of Mφs and the entire immune system (Abbas et al., 2015). Only compound **1**, at a single, not the highest concentration (10^{-5} moldm^{-3}), produced a statistically significant decrease in cell adherence (Fig. 6). The positive control used in the viability assays, cisplatin, did not alter this Mφ ability, which is in accordance with previous results (Radulović et al., 2017). We already noted that compound **1** showed a potentiating effect on the uptake/retention of NR, which is directly linked to the functioning of the membrane of lysosomes. Cell adherence is likewise inherently connected to the cell membrane functioning, and we could expect that similar effects could be expressed on both the lysosomal and cell membranes, i.e. that the cell membrane stability and consequently the adherence ability are enhanced. At this concentration (10^{-5}

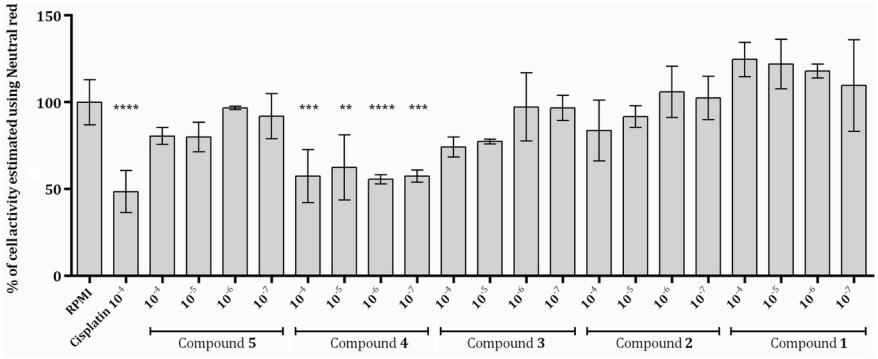

Fig. 5. The effects of compounds **1–5** (in moldm^{-3}) on Mφ survival ability estimated by the Neutral red assay. Data are presented as mean ± S.D. The statistical significance was calculated by one-way ANOVA followed by Dunnett's post-hoc test. **p < 0.01, ***p < 0.001 and ****p < 0.0001 vs. RPMI medium-treated cells.

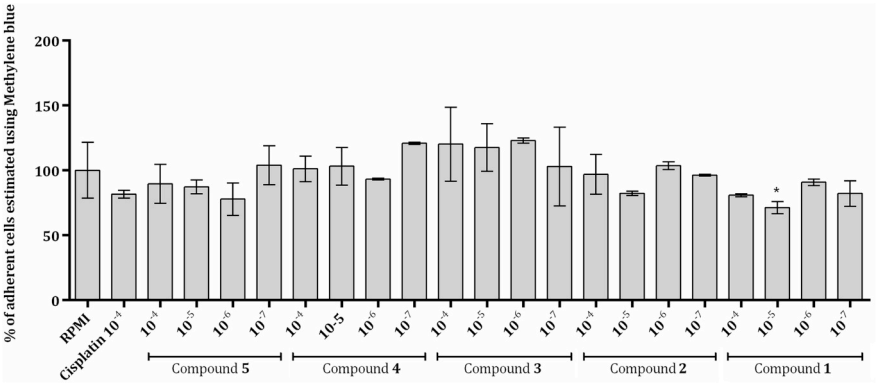

Fig. 6. The effects of compounds **1–5** (in moldm^{-3}) on Mφ adherence ability estimated using the methylene-blue assay. Data are presented as mean ± S.D. The statistical significance was calculated by one-way ANOVA followed by Dunnett's post-hoc test. *p < 0.05 vs. RPMI medium-treated cells.

moldm^{-3}) compound **1** had not shown any toxicity in the MTT assay. Upon concentration increase to 10^{-4} moldm^{-3}, compound **1** might only appear to have no effect on Mφ adherence, as the outcome could, in fact, be the result of two opposing effects, reduction in cell viability and enhancement of the membrane effects.

The main function of myeloperoxidase (MPO), an enzyme present in phagocytes, is the generation of microbicidal HOCl. High amounts of MPO are present in neutrophil azurophilic granules, which are mobilized into the phagolysosome vacuole during phagocytosis. MPO is also present in monocytes and macrophages, although to a lesser degree than in neutrophils (de Araujo et al., 2013). Compounds **1**, **3** and **4** decreased the MPO enzymatic activity in rat peritoneal macrophages in a statistically significant manner (Fig. 7). Namely, the MPO activity was reduced in the presence of the lowest tested concentrations of compounds **1** and **4,** or at the same concentration (compound **3**) as cisplatin. However, compounds **2** and **5** did not significantly affect MPO activity in any of the tested concentrations. Previously, immunomodulatory effects of higher concentrations of a crude ethanolic extract of *Didemnum albidum* on human macrophages were demonstrated (Ananthan and Iyappan, 2014). However, this extract showed a stimulating effect on lysosomal enzyme activity (Ananthan and Iyappan, 2014), which is contrary to our results obtained for MPO (lysosomal protein) activity.

However, the observed discrepancy could be the outcome of the comparison of the result of different methods, since the total cellular lysosomal enzyme activity was determined by an acid phosphatase method, while we selectively measured MPO activity. Also, the effects of crude extracts could be different from that of the individual compound(s) and a direct comparison of the results could be misleading, especially when no chemical analysis accompanying the biological tests exists, like in the case of the study of Ananthan et al. (2011).

2.2.4. The appearance of Mφs under the influence of the tested compounds

Finally, we wanted to verify/visualize the observed influence of the tested compounds in the abovementioned assay, and the microscopic appearance of the treated Mφs was investigated as well. Under the inverted microscope lens, Mφs cultured in RPMI appeared mostly as round cells, with occasional spindle-like cells (Fig. 8A). The treatment with compound **1**, in the highest concentration, lead to cell swelling (Fig. 8B), possibly due to the impact on cell membrane function and/or cell necrosis, and an increase in cell debris. Similar findings, but with a certain number of apoptotic cells observed, were seen in Mφs exposed to cisplatin (Fig. 8C).

Liberio et al. (2014) tested 143 ascidian extracts on the breast cancer cell line MDA-MB-231 and found that 21 of them possessed cytotoxic activity. A number of the tested extracts produced noted changes only after several days of incubation with the cells and the authors explained such delayed action by metabolic activation, accumulation in the cells, toxic intermediates, etc. (Liberio et al., 2014). One should have in mind that the mentioned study was done on cancer cells with a high proliferative index, where cytotoxicity is a desirable effect. In this work, we tested a selected ascidian metabolite and related compounds on normal cells of the immune system where cytotoxicity could be regarded as a drawback. Thus, potential anticancer compounds should exert a cytotoxic effect on malignant cells while having no or minimal effect of normal healthy cells, like Mφs. In our study, based on the MTT test results, compounds **1–5** were shown to be safe for Mφs at concentrations lower than 5×10^{-5} moldm^{-3}. However, the obtained results should be taken with caution, as cytotoxicity of ascidian extracts was observed even after 48 h or more, and all our tests with Mφs lasted only for 24 h (Liberio et al., 2014).

One can conclude that the tested tyramides exert a varying degree of toxicity towards brine shrimps, and in some cases, the determined LD_{50} concentrations were even lower than those of known toxicants (e.g.

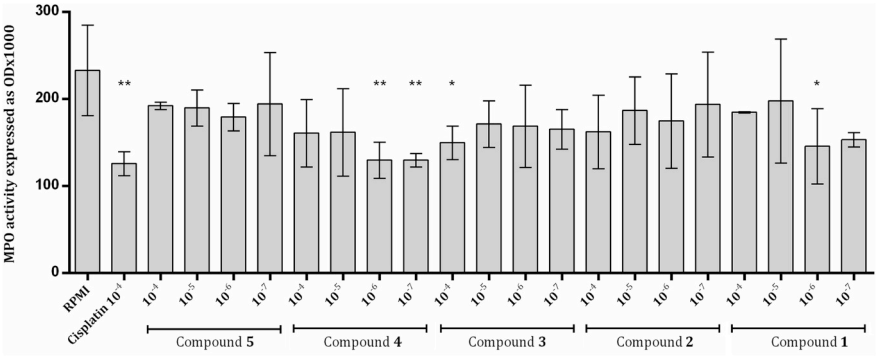

Fig. 7. The effects of compounds **1–5** (in moldm^{-3}) on macrophage MPO activity. Data are presented as mean ± S.D. The statistical significance was calculated by one-way ANOVA followed by Dunnett's post-hoc test. *p < 0.05 and **p < 0.01 vs. RPMI medium-treated cells.

Fig. 8. Cell appearance in RPMI medium (A) and after the treatment with compound **1** (B) and cisplatin (C), at the concentration of 10^{-4} M, at a magnification × 100.

strychnine sulfate, SDS). The toxicity was highly dependent on the structure of these mutually related compounds, while the natural one, isolated from a marine species (the ascidian *Didemnum rubeum*), was shown to be the most toxic one. The presence and the location of iodine atoms in the molecules could be brought into connection with the observed effects. In the case of macrophage cultures, the tested tyramides were much less toxic but were found to have an effect on the functioning of these normal cells, most probably by interfering with the function of cell membranes and changing the reducing cellular capacity. One can only speculate that the natural metabolite **1** contributes to the previously noted cytotoxic activity of a water ascidian extract known to contain this compound (Solano et al., 2009). Prompted by such selective toxicity, further work in this direction seems necessary and justified as immunomodulatory compounds not affecting macrophage viability but modulating their function are of interest.

3. Materials and methods

3.1. Synthesis and spectral characterization

3.1.1. Chemicals

All commercially available chemicals were acquired from Sigma-Aldrich (USA), Merck (Germany), Fluka (Germany) and Carl Roth (Germany), and used as received with the exception of solvents that were additionally dried and purified by distillation.

3.1.2. Methods

All reactions were performed in oven-dried (120 °C) glassware under an atmosphere of dry nitrogen. ^{1}H and ^{13}C NMR spectra were recorded on a Bruker Avance III spectrometer (Bruker, Fällanden, Switzerland) operating at 400 and 100.6 MHz, respectively. 2D experiments (ROESY, NOESY and gradient ^{1}H–^{1}H COSY, HSQC, HMBC), as well as DEPT-90, DEPT-135 and selective ^{1}H homonuclear decoupling measurements, were run on the same instrument with the built-in Bruker pulse sequences. All NMR spectra were measured at 25 °C in $CDCl_3$ with tetramethylsilane as an internal standard. Chemical shifts were reported as δ values in parts per million (ppm). Scalar couplings (*J*) are reported in Hertz. GC-MS analyses were performed on a Hewlett-Packard 6890N gas chromatograph equipped with a fused silica capillary column HP-5MS (5% phenylmethylsiloxane, 30 m × 0.25 mm, film thickness 0.25 μm, Agilent Technologies, USA) and coupled with a 5975B mass selective detector from the same company. The injector and interface were operated at 250 °C and 320 °C, respectively. Oven temperature was raised from 150 to 310 °C at a heating rate of 5 °C/min and then isothermally held for 10 min. As a carrier gas, He at 1.0 mL/min was used. The samples (1 μL of the corresponding solutions in $CHCl_3$ (1 mg per 1 mL)) were injected in a pulsed-split mode (the flow was 1.5 mL/min for the first 0.5 min and then set to 1.0 mL/min throughout the rest of the analysis: split ratio, 40:1). MS conditions: ionization voltage 70 eV, acquisition mass range, 35–650 amu, scan time, 0.32 s. Silica gel 60, particle size distribution 40–63 mm, was used for column chromatography. Thin layer chromatography (TLC) was performed on Merck plates (Darmstadt, Germany), layer thickness 0.2 mm with silica gel 60 and fluorescence indicator F_{254}. Visualization was accomplished with UV light (254 nm) or by spraying with 50% (*v*/*v*) aqueous H_2SO_4, followed by 2-min heating at 110 °C. IR measurements (ATR-attenuated total reflectance) were carried out using an FT-IR instrument model 6700 (Thermo Nicolet, Waltham, USA). UV spectra (in acetonitrile) were measured using a UV-1800 spectrophotometer (Shimadzu, Tokyo, Japan). Melting points were determined on MPM-HV2 melting point meter (Paul Marienfeld GmbH & Co. KG, Lauda-Königshofen, Germany). Microanalysis of carbon, nitrogen, and hydrogen were carried out on a Carlo Erba Elemental Analyzer model 1106 (Carlo Erba Strumentazione, Milan, Italy) and their results agreed favorably with the calculated values.

3.1.3. Synthesis of N-(4-methoxyphenethyl)benzamide (4) and N-(4-methoxyphenethyl)formamide (6)

A solution of 2-(4-methoxyphenyl)ethanamine (1.00 g, 6.6 mmol), 4-(dimethylamino)pyridine (DMAP, 30 mg), *N*,*N*′-dicyclohexylcarbodiimide (DCC, 1.50 g, 7.3 mmol), and benzoic (1.21 g, 9.9 mmol) or formic acid (95% *w*/*w*, 474 mg, 9.8 mmol) in dry CH_2Cl_2 (20 mL) was stirred overnight at room temperature protected from atmospheric moisture by a $CaCl_2$ guard tube. In the case of formamide formation, since the used formic acid contained up to 5% of water, the reaction mixture additionally included solid anhydrous $MgSO_4$ (2 g). Workup: silica gel (5 g) was added to the obtained suspension, dichloromethane removed *in vacuo*, and the residue dry-loaded onto an already packed column of SiO_2. Gradient elution of the column with ternary mixtures of hexane, diethyl ether and dichloromethane (from 1:1:1 to 1:1:2, *v*/*v*) gave pure **4** and **6** in 75% and 83%, respectively.

3.1.3.1. N-(4-Methoxyphenethyl)benzamide (4). White crystalline substance; MP 120.7 °C (lit. 123–124 °C, Kincl et al., 1956); Calc. for $C_{16}H_{17}NO_2$: C, 75.27; H, 6.71; N, 5.49; O, 12.53%. Found: C, 75.12; H, 6.78; N, 5.42; O, 12.68%; FTIR (neat) ν_{max}/cm^{-1} 3314, 3080, 2931, 2833, 1633, 1536, 1510, 1240, 814, 754, 692; UV λ_{max} (CH_3CN)/nm 283.2 (log ε 3.37), 275.8 (3.49), 225.2 (4.41) and 194.2 (5.04); retention time (HP-5MS) = 11.835 min, EI-MS *m*/*z* (rel. intensity, %): 255 (M^+, 1.5%), 135 (10.1), 134 (100), 121 (20.6), 105 (30.6), 78 (5.3), 77 (21.9), 51 (4.6). For ^{1}H and ^{13}C NMR spectra, see Tables 1 and 2 (Liao et al., 1988).

3.1.3.2. N-(4-Methoxyphenethyl)formamide (6). White amorphous solid; Calc. for $C_{10}H_{13}NO_2$: C, 67.02; H, 7.31; N, 7.82; O, 17.85%. Found: C, 67.12; H, 7.20; N, 7.78; O, 17.90%; FTIR (neat) ν_{max}/cm^{-1} 3286, 3080, 2934, 2836, 1654, 1611, 1510, 1440, 1241, 810, 752; UV λ_{max} (CH_3CN)/nm 283.4 (log ε 3.14), 276.8 (3.21), 224.6 (3.99) and 195.0 (4.65); retention time (HP-5MS) = 5.805 min, EI-MS *m*/*z* (rel. intensity, %): 179 (M^+, 3.7%), 135 (10.3), 134 (100), 121 (76.9), 119 (8.2), 91 (9.5), 77 (10.9), 51 (3.3). For ^{1}H and ^{13}C NMR spectra, see Tables 1 and 2.

3.1.4. Iodination of compounds 4 and 6

A mixture of amide **4** or **6** (0.7 mmol), mercury(II) acetate (0.55 g, 1.73 mmol) and one drop of 70% (*w*/*w*) perchloric acid in 14 mL of

glacial acetic acid was stirred for 48 h at room temperature. The reaction was quenched with 31 mL saturated solution of sodium chloride in water and subsequently stirred additionally for 30 min at room temperature. The precipitated arylmercuric chlorides were centrifuged and dried under reduced pressure. Then, the stirred suspension of the crude arylmercuric chlorides in dry CH_2Cl_2 (20 mL) was treated with a solution of iodine (0.44 g, 1.73 mmol) in 10 mL dry dichloromethane. The stirring was continued for 16 h and then the precipitate was filtered off. The filtrate was washed with sodium thiosulfate solution and water, dried over anh. $MgSO_4$ and the solvent evaporated. The crude products (mixtures of mono and diiodinated benzamide and formamide derivatives) were separated by an isocratic column chromatography using hexane/diethyl ether/dichloromethane (3:1:1 or 1:1:1, respectively).

*3.1.4.1. N-(3,5-Diiodo-4-methoxyphenethyl)benzamide **(1)***. White crystalline substance; MP 127.7 °C; Calc. for $C_{16}H_{15}I_2NO_2$: C, 37.90; H, 2.98; I, 50.05; N, 2.76; O, 6.31%. Found: C, 37.78; H, 2.85; N, 2.78%; FTIR (neat) ν_{max}/cm^{-1} 3280, 3060, 2928, 1628, 1533, 1458, 1245, 995, 866, 692; UV λ_{max} (CH_3CN)/nm 288.4 (log ε 3.45), 222.6 (4.64), and 193.0 (4.90); retention time (HP-5MS) = 18.131 min, EI-MS *m/z* (rel. intensity, %): 507 (M^+, 0.7), 386 (100), 380 (23.3), 373 (6.8), 260 (13.9), 246 (1.9), 244 (3.6), 207 (5.9), 105 (91.5), 77 (38.9), 51 (7.6). For ^1H and ^{13}C NMR spectra, see Tables 1 and 2.

*3.1.4.2. N-(2,5-Diiodo-4-methoxyphenethyl)benzamide **(2)***. White crystalline substance; MP 192 °C; Calc. for $C_{16}H_{15}I_2NO_2$: C, 37.90; H, 2.98; I, 50.05; N, 2.76; O, 6.31%. Found: C, 37.82; H, 2.96; N, 2.73%; FTIR (neat) ν_{max}/cm^{-1} 3293, 3080, 2910, 2830, 1625, 1540, 1478, 1243, 1052, 880, 830, 692, 595; UV λ_{max} (CH_3CN)/nm 298.0 (log ε 3.98), 241.0 (4.68), 213.6 (4.93) and 193.0 (5.12); retention time (HP-5MS) = 18.201 min, EI-MS *m/z* (rel. intensity, %): 507 (M^+, 0.7), 387 (9.6), 386 (100), 380 (25.7), 373 (7.5), 260 (3.8), 105 (80.3), 77 (35.2), 51 (6.4). For ^1H and ^{13}C NMR spectra, see Tables 1 and 2.

*3.1.4.3. N-(3-Iodo-4-methoxyphenethyl)benzamide **(3)***. White crystalline substance; MP 141.2 °C; Calc. for $C_{16}H_{16}INO_2$: C, 50.41; H, 4.23; I, 33.29; N, 3.67; O, 8.39%. Found: C, 50.53; H, 4.15; N, 3.70%; FTIR (neat) ν_{max}/cm^{-1} 3241, 3090, 2930, 2830, 1630, 1538, 1489, 1250, 860, 807, 697, 595; UV λ_{max} (CH_3CN)/nm 283.0 (log ε 3.77), 225.0 (4.72) and 194.0 (5.12); retention time (HP-5MS) = 15.502 min, EI-MS *m/z* (rel. intensity, %): 381 (M^+, 0.4), 260 (100), 247 (8.0), 245 (6.0), 134 (1.4), 118 (2.2), 105 (44.5), 77 (25.4), 51 (5.7). For ^1H and ^{13}C NMR spectra, see Tables 1 and 2.

*3.1.4.4. N-(2-Iodo-4-methoxyphenethyl)benzamide **(7)***. Retention time (HP-5MS) = 15.142 min, EI-MS *m/z* (rel. intensity, %): 381 (M^+, 0.9), 260 (100), 254 (9.1), 247 (14.6), 134 (1.4), 120 (6.1), 105 (55.4), 91 (4.1), 77 (27.7), 51 (6.8). For ^1H and ^{13}C NMR spectra, see Tables 1 and 2.

*3.1.4.5. N-(3-Iodo-4-methoxyphenethyl)formamide **(5)***. White crystalline substance; MP 80.5 °C; Calc. for $C_{16}H_{16}INO_2$: C, 39.36; H, 3.96; I, 41.59; N, 4.59; O, 10.49%. Found: C, 39.41; H, 3.85; N, 4.55%; FTIR (neat) ν_{max}/cm^{-1} 3274, 3021, 2939, 2865, 1647, 1372, 1250, 865, 812, 763, 594; UV λ_{max} (CH_3CN)/nm 290.2 (log ε 2.21), 283.0 (2.23), 204.6 (3.24) and 198.2 (3.25); retention time (HP-5MS) = 10.039 min, EI-MS *m/z* (rel. intensity, %): 305 (M^+, 4,5), 260 (100), 247 (32.1), 245 (8.4), 231 (1.2), 118 (3.6), 90 (14.6), 77 (12.5), 51 (3.3). For ^1H and ^{13}C NMR spectra, see Tables 1 and 2.

*3.1.5. Synthesis of 4-hydroxy-3,5-diiodobenzaldehyde **(8)***

To a well stirred, cooled (12–15 °C) suspension of 4-hydroxybenzaldehyde (3.00 g, 24.6 mmol) in aqueous sodium hydrogencarbonate (3.10 g, 36.9 mmol, $NaHCO_3$ in 20 mL of water), solid pulverized iodine (6.2 g, 24.6 mmol) was added in small portions. Stirring was continued for 30 min at room temperature, and then the reaction mixture was neutralized with HCl solution (10%, *w/w*), and extracted with ethyl acetate. The dried (anh. $MgSO_4$) ethyl acetate phase was evaporated *in vacuo*. 4-Hydroxy-3-iodobenzaldehyde was taken up in diethyl ether from the solid residue. The remaining white solid represented pure 4-hydroxy-3,5-diiodobenzaldehyde. Yield for **8** was 1.0 g (29%). ^1H NMR spectrum of the obtained pure substance corresponded to literature values (Kiran et al., 2006); see Supplementary data file.

*3.1.6. Synthesis of 3,5-diiodo-4-methoxybenzaldehyde **(9)***

Methyl iodide (0.4 g, 2.8 mmol) was added to a suspension of 4-hydroxy-3,5-diiodobenzaldehyde (**8**, 1.0 g, 2.7 mmol) and anhydrous potassium carbonate (0.75 g, 5.5 mmol) in dry *N*,*N*-dimethylformamide (10 mL). After 24 h of stirring at room temperature, water (40 mL) was added and the obtained mixture extracted with Et_2O (50 mL, 3 ×). The combined organic layers were washed excessively with brine, and the formamide-free ether solution dried over anhydrous $MgSO_4$ and the solvent evaporated. Yield for **9** was 0.72 g (69.2%); for experimental data see the Supplementary file.

3.2. Toxicological/pharmacological assays

3.2.1. Drugs and chemicals used in pharmacological assays

Cell culture medium (RPMI medium, acquired from Sigma-Aldrich, St. Louis, MO, USA) used for cell-related experiments consisted of RPMI 1640 with 20 mmoldm^{-3} HEPES and L-glutamine, without sodium bicarbonate, containing 5% (*w/v*) fetal bovine serum, 200 mgmL^{-1} streptomycin (AppliChem, Darmstadt, Germany) and 200 IU mL^{-1} penicillin (AppliChem, Darmstadt, Germany). Cisplatin, a standard cytotoxic drug, was acquired from Teva (Belgrade, Serbia) and 3-(4,5-dimethylthiazol-2-yl)-2,5-diphenyltetrazolium bromide (MTT) used for cell viability determination was obtained from Sigma-Aldrich (St. Louis, MO, USA).

3.2.2. Acute toxicity – Artemia salina model

Acute toxicity in *Artemia salina* was evaluated using the method previously described by Radulović et al. (2013). Final concentrations of the tested samples dissolved in aqueous dimethyl sulfoxide (DMSO) were as follows: 1–200 μM, whereas the final concentration of DMSO was much less than 1% (*v/v*). DMSO was inactive under the started conditions as demonstrated by a negative control. Dead nauplii were counted after 24 and 48 h. All tests were performed in triplicate. LC_{50} (concentration lethal to 50% of nauplii) were determined after statistical analysis. Sodium dodecyl sulfate (SDS) was used as the positive control.

3.2.3. Animal housing, cell isolation, and cultivation

In this experiment male and female Wistar rats (250–300 g) were used. The animals were housed under standard laboratory conditions (temperature 22 ± 2 °C, humidity 60%, with food and water available *ad libitum*) in the Vivarium of the Institute of Biomedical Research, at the Medical Faculty, University of Niš. All experimental procedures with the animals were conducted in compliance with the declaration of Helsinki and European Community guidelines for the ethical handling of laboratory animals (EU Directive of 2010; 2010/63/EU) and were also approved by the local Ethics Committee (No. 323-07-06862/2016-05/2).

Rats were intraperitoneally injected with thioglycolic acid, as described previously, in order to induce recruitment of circulatory monocytes and proliferation of resident peritoneal macrophages (Radulović et al., 2014, 2017). Elicited peritoneal macrophages (Mφs) were isolated following previously described standard procedures and viable cell suspensions (determined using trypan blue staining; > 95% of viable cells) were set to 2.5 × 10^6 viable cells per mL. Cells were transferred to 96-well microtiter plates and allowed to adhere to the surface for 1.5 h at 37 °C under 5% (*v/v*) CO_2 atmosphere.

3.2.4. Macrophage ability to metabolize MTT (Viability assay)

After the initial step of adherence, Mφs were exposed to different concentrations of cisplatin (4×10^{-8}–7×10^{-6} moldm^{-3}) or compounds **1–5** in concentrations that were water soluble (ranging from 10^{-7} to 5×10^{-4} moldm^{-3}), dissolved in RPMI medium, and further incubated for 24 h at 37 °C under 5% (*v/v*) CO_2 atmosphere. Cell viability was checked after the incubation period using a standard MTT (5 mgmL^{-1}) assay (Radulović et al., 2017). The formation of formazan crystals, 4 h later, was evaluated and the absorbance of each well was recorded at 540 nm (Multiscan Ascent, Labsystems, Finland). The activity of the tested compounds was expressed as % of viability based on the formed formazan crystals relative to the one produced by the RPMI-medium cultured cells. All experiments were done in triplicate and repeated three times.

3.2.5. Evaluation of macrophage functional properties

3.2.5.1. Neutral red assay (Lysosomal function evaluation). This assay utilizes neutral red (NR), a dye which penetrates into normal lysosomes and stains them (Radulović et al., 2017). Briefly, after a 24-h incubation period with the tested compounds, following the protocol described in the previous section, the medium was removed, cells washed and incubated with NR for an additional 2 h. After that, excess dye was removed, the plates were washed and a destaining solution (ethanol: water: acetic acid = 5:5:1, *v/v/v*) was added. The amount of the extracted/remaining dye was measured at 540 nm. The obtained results were presented as % of cells ability to retain NR relative to the same ability of RPMI-medium cultured cells. All experiments were done in triplicate and repeated three times.

3.2.5.2. Methylene blue assay (Adherence ability evaluation). The adherence ability of Mφs, exposed to cisplatin or compounds **1–5** in the same concentrations as described in section 3.2.4, was evaluated using a methylene blue-staining protocol (Radulović et al., 2017). The treatment was performed during the initial step of Mφ adherence for 1.5 h. After this period, cells were fixed in methanol and stained for 30 min with 1% (w/v) methylene blue solution. Excess dye was removed by a subsequent wash with distilled water and the remaining cell-retained dye was extracted using a mixture of ethanol and 0.1 moldm^{-3} hydrochloric acid (1:1, *v/v*). The absorbance of the extracts from each well was recorded at 620 nm and the results are presented as % of adhered cells relative to the absorbance measured for the RPMI-medium cultured cells. All experiments were done in triplicate and repeated three times.

3.2.5.3. Myeloperoxidase (MPO) activity determination. Primary Mφ cultures were exposed to cisplatin and compounds **1–5** in the same concentrations as described in section 3.2.4. The activity of MPO was determined using 1,2-diaminobenzene as a color reagent and the enzymatic reaction was initiated with the addition of H_2O_2 (Radulović et al., 2014). The reaction was stopped with an H_2SO_4 solution (1 M) and the optical densities (ODs) of the formed product were determined at 540 nm. The results are expressed as ODs (absorbance at 540 nm) × 1000. All experiments were done in triplicate and repeated three times.

3.2.5.4. Microscopic examination of Mφs. After 24 h of incubation of Mφs exposed to cisplatin and compounds **1–5**, the cells were observed using a light microscope Zeiss Z1 AxioObserver (Carl Zeiss, Göttingen, Germany), with optical magnifications of 100 and 200. Changes in the number, shape and morphological characteristics of Mφs were observed and described.

3.3. Statistical analysis

The results of biological assays were expressed as the mean ± S.D. Statistically significant differences were determined by one-way analysis of variance (One-Way ANOVA) followed by Dunnett's post-hoc test for multiple comparisons (GraphPad Prism version 5.03, San Diego, CA, USA). Probability values (p) less than 0.05 were considered statistically significant.

Conflict of interest declaration

The authors declare no conflict of interest.

Acknowledgment

This work was supported by the Ministry of Education, Science and Technological Development of the Republic of Serbia (Project No. 172061). This study is a part of the Ph.D. thesis of Miljana R. Đorđević under the supervision of Niko S. Radulović.

Appendix A. Supplementary data

Supplementary data to this article can be found online at https://doi.org/10.1016/j.fct.2018.12.039.

Transparency document

Transparency document related to this article can be found online at https://doi.org/10.1016/j.fct.2018.12.039.

References

Abbas, A., Lichtman, A.H., Pillai, S., 2015. Cellular and Molecular Immunology, eighth ed. Elsevier/Saunders, Philadelphia.

Abdul Jaffar Ali, H., Tamilselvi, M., 2016. Ascidians in Coastal Water: a Comprehensive Inventory of Ascidian Fauna from the Indian Coast. Springer International Publishing, Switzerland. https://doi.org/10.1007/978-3-319-29118-5.

Aiello, A., Fattorusso, E., Imperatore, C., Menna, M., Müller, W.E.G., 2010. Iodocionin, a cytotoxic iodinated metabolite from the Mediterranean ascidian *Ciona edwardsii*. Mar. Drugs 8, 285–291. https://doi.org/10.3390/md8020285.

Ananthan, G., Iyappan, K., 2014. Immunomodulatory activity of ethanol extract of the ascidian *Didemnum albidum*. World J. Pharm. Pharmaceut. Sci. 3, 745–755.

Ananthan, G., Sivaperumal, P., Hussain, S.M., 2011. Cytotoxicity of the crude extracts of marine ascidians (Tunicata: Ascidiacea) from Tuticorin, Southeast coast of India. Arch. Appl. Sci. Res. 3, 139–142.

Borrelli, F., Campagnuolo, C., Capasso, R., Fattorusso, E., Taglialatela-Scafati, O., 2004. Iodinated indole alkaloids from *Plakortis simplex* – new plakohypaphorines and an evaluation of their antihistamine activity. Eur. J. Org. Chem. 3227–3232. https://doi.org/10.1002/ejoc.200400181. 2004.

Carroll, A.R., Bowden, B.F., Coll, J.C., 1993. Studies of Australian ascidians. II. Novel cytotoxic iodotyrosine-based alkaloids from colonial ascidians, *Aplidium* sp. Aust. J. Chem. 46, 825–832. https://doi.org/10.1071/ch9930825.

Coombe, D.R., Ey, P.L., Schluter, S.F., Jenkin, C.R., 1981. An agglutinin in the haemolymph of an ascidian promoting adhesion of sheep erythrocytes to mouse macrophages. Immunology 42, 661–669.

Davidson, B.S., 1993. Ascidians: producers of amino acid derived metabolites. Chem. Rev. 93, 1771–1791. https://doi.org/10.1021/cr00021a006.

de Araujo, T.H., Okada, S.S., Ghosn, E.E., Taniwaki, N.N., Rodrigues, M.R., de Almeida, S.R., Mortara, R.A., Russo, M., Campa, A., Albuquerque, R.C., 2013. Intracellular localization of myeloperoxidase in murine peritoneal B-lymphocytes and macrophages. Cell. Immunol. 281, 27–30. https://doi.org/10.1016/j.cellimm.2013.01.002.

Dugrillon, A., Gaetner, R., 1995. δ-Iodolactones decrease epidermal growth factor-induced proliferation and inositol-1,4,5-trisphosphate generation in porcine thyroid follicles-a possible mechanism of growth inhibition by iodide. Eur. J. Endocrinol. 132, 735–743. https://doi.org/10.1530/eje.0.1320735.

Fayette, J., Coquard, I.R., Alberti, L., Ranchère, D., Boyle, H., Jean-Yves Blay, J.-Y., 2005. ET-743: a novel agent with activity in soft tissue sarcomas. Oncol. 10, 827–832. https://doi.org/10.1634/theoncologist.10-10-827.

González-Santiago, L., Suárez, Y., Zarich, N., Muñoz-Alonso, M.J., Cuadrado, A., Martínez, T., Goya, L., Iradi, A., Sáez-Tormo, G., Maier, J.V., Moorthy, A., Cato, A.C., Rojas, J.M., Muñoz, A., 2006. Aplidin® induces JNK-dependent apoptosis in human breast cancer cells via alteration of glutathione homeostasis, Rac1 GTPase activation, and MKP-1 phosphatase downregulation. Cell Death Differ. 13 (11), 1968–1981. https://doi.org/10.1038/sj.cdd.4401898.

Irsfeld, M., Spadafore, M., Prüß, B.M., 2013. β-Phenylethylamine, a small molecule with a large impact. Webmedcentral 4, 4409. https://doi.org/10.9754/journal.wmc.2013.004459.

Itoh, N., Tsujita, M., Ando, T., Hisatomi, G., Higashi, T., 1997. Formation and emission of monohalomethanes from marine algae. Phytochemistry 45, 67–73. https://doi.org/10.1016/s0031-9422(96)00786-8.

Kazlauskas, R., Murphy, P.T., Wells, R.J., Baird-Lambert, J.A., Jamieson, D.D., 1983.

Halogenated pyrrolo[2,3-*d*]pyrimidine nucleosides from marine organisms. Aust. J. Chem. 36, 165–170. https://doi.org/10.1071/ch9830165.
Kigoshi, H., Kanematsu, K., Uemura, D., 1999. Turbotoxins A and B, novel diiodotyramine derivatives from the Japanese gastropod *Turbo marmorata*. Tetrahedron Lett. 40, 5745–5748. https://doi.org/10.1016/s0040-4039(99)01099-0.
Kincl, F.A., Romo, J., Rosenkranz, G., Sondheimer, F., 1956. The constituents of *Casimiroa edulis* llave et lex. Part I. The seed. J. Chem. Soc. 0, 4163–4169. https://doi.org/10.1039/JR9560004163.
Kiran, Y.B., Konakahara, T., Sakai, N., 2006. A green reagent for the iodination of phenols. Synthesis 15, 2327–2332. https://doi.org/10.1055/s-2008-1078598.
Lambert, G., Karney, R.C., Rhee, W.Y., Carman, M.R., 2016. Wild and cultured edible tunicates: a review. Manag. Biol. Invasions 7, 59–66. https://doi.org/10.3391/mbi.2016.7.1.08.
Liao, L., Li, G., Li, J., Yang, C., Zhou, J., 1988. Chemical constituents of *Z. myriacanthum* and chemotaxonomy of *Zanthoxyllum*. Acta Bot. Yunnanica 10, 445–456.
Liberio, M.S., Sadowski, M.C., Nelson, C.C., Davis, R.A., 2014. Identification of eusynstyelamide B as a potent cell cycle inhibitor following the generation and screening of an ascidian-derived extract library using a real time cell analyzer. Mar. Drugs 12, 5222–5239. https://doi.org/10.3390/md12105222.
Meyer, B.N., Ferrigni, N.R., Putnam, J.E., Jacobsen, L.B., Nichols, D.E., McLaughlin, J.L., 1982. Brine shrimp: a convenient general bioassay for active plant constituents. Planta Med. 45, 31–34. https://doi.org/10.1055/s-2007-971236.
Murphy, C.D., 2003. New frontiers in biological halogenation. J. Appl. Microbiol. 94, 539–548. https://doi.org/10.1046/j.1365-2672.2003.01900.x.
Palanisamy, S.K., Rajendran, N.M., Marino, A., 2017. Natural products diversity of marine ascidians (Tunicates; Ascidiacea) and successful drugs in clinical development. Nat. Prod. Bioprospect. 7, 1–111. https://doi.org/10.1007/s13659-016-0115-5.
Pfaffenbach, M., Gaich, T., 2015. A photoinduced cyclization cascade-total synthesis of (-)-leuconoxine. Chem. Eur J. 21, 6355–6357. https://doi.org/10.1002/chem.201500656.
Radulović, N.S., Đorđević, M.R., Blagojević, P.D., 2016a. Structural revision of aristol: a fresh look at the oxidative coupling of thymol under iodination conditions. RSC Adv. 6, 69067–69082. https://doi.org/10.1039/c6ra11296j.
Radulović, N.S., Filipović, S.I., Zlatković, D.B., Đorđević, M.R., Stojanović, N.M., Ranđelović, P.J., Mitić, K.V., Jevtović-Stoimenov, T.M., Ranđelović, V.N., 2016b. Immunomodulatory pinguisane-type sesquiterpenes from the liverwort *Porella cordaeana* (Porellaceae): the “new old” furanopinguisanol and its oxidation product exert mutually different effects on rat splenocytes. RSC Adv. 6, 41847–41860. https://doi.org/10.1039/c6ra04308a.
Radulović, N.S., Mladenović, M.Z., Blagojević, P.D., Stojanović-Radić, Z.Z., Ilić-Tomić, T., Senerović, L., Nikodinović-Runić, J., 2013. Toxic essential oils. Part III: identification and biological activity of new allylmethoxyphenyl esters from a Chamomile species (*Anthemis segetalis* Ten.). Food Chem. Toxicol. 62, 554–565. https://doi.org/10.1016/j.fct.2013.09.017.
Radulović, N.S., Todorovska, M.M., Zlatković, D.B., Stojanović, N.M., Ranđelović, P.J., 2017. Two goitrogenic 1,3-oxazolidine-2-thione derivatives from Brassicales taxa: challenging identification, occurrence and immunomodulatory effects. Food Chem. Toxicol. 110, 94–108 doi:S0278-6915(17)30583-5.
Radulović, N.S., Zlatković, D.B., Mitić, K.V., Randjelović, P.J., Stojanović, N.M., 2014. Synthesis, spectral characterization, cytotoxicity and enzyme-inhibiting activity of new ferrocene–indole hybrids. Polyhedron 80, 134–141. https://doi.org/10.1016/j.poly.2014.03.006.
Restrepo, M.P., Surmay, V.S., Jaramillo, E.G., Restrepo, S.R., 2019. Anti-parasite activity of novel 3,5-diiodophenethyl-benzamides. J. Braz. Chem. Soc. 30, 116–123. https://doi.org/10.21577/0103-5053.20180160.
Shenkar, N., Swalla, B.J., 2011. Global diversity of Ascidiacea. PLoS One 6https://doi.org/10.1371/journal.pone.0020657. e20657-e.
Solano, G., Motti, C.A., Jaspars, M., 2009. New iodotyramine derivatives from *Didemnum rubeum*. Tetrahedron 65, 7482–7486. https://doi.org/10.1016/j.tet.2009.07.002.
Sri Kumaran, N., Bragadeeswaran, S., Meenakshi, V.K., 2011. Evaluation of antibacterial activity of crude extracts of ascidian *Didemnum psammathodes* Sluiter, 1895 against isolated human and fish pathogens. Asian Pac. J. Trop. Biomed. 1, S90–S99. https://doi.org/10.1016/S2221-1691(11)60132-9.
Suzuki, O., Katsumata, Y., Oya, M., 1981. Oxidation of beta-phenylethylamine by both types of monoamine oxidase: examination of enzymes in brain and liver mitochondria of eight species. J. Neurochem. 36, 1298–1301. https://doi.org/10.1111/j.1471-4159.1981.tb01734.x.
Toğulga, M., 1998. The short-term toxicity of two toxicants to Artemia Nauplii. Tr. J. Zool. 22, 259–266.
Watters, D.J., 2018. Ascidian toxins with potential for drug development. Mar. Drugs 16, E162. https://doi.org/10.3390/md16050162.
Williams, P.G., Yoshida, W.Y., Moore, R.E., Paul, V.J., 2003. Novel iodinated diterpenes from a marine cyanobacterium and red alga assemblage. Org. Lett. 5, 4167–4170. https://doi.org/10.1021/ol035620u.
Won, T.H., Kim, C.K., Lee, S.H., Rho, B.J., Lee, S.K., Oh, D.C., Oh, K.B., Shin, J., 2015. Amino acid-derived metabolites from the ascidian *Aplidium* sp. Mar. Drugs 13, 3836–3848. https://doi.org/10.3390/md13063836.